Journal of Magnetics 18(2), 173-177 (2013)

ISSN (Print) 1226-1750
ISSN (Online) 2233-6656
http://dx.doi.org/10.4283/JMAG.2013.18.2.173

Development of High-Sensitivity Cantilever-Detected ESR Measurement Using a Fiber-Optic Interferometer

Yuki Tokuda[1], Daichi Tsubokura[1], Eiji Ohmichi[1]*, and Hitoshi Ohta[2]

[1]*Graduate School of Science, Kobe University, Kobe 657-8501, Japan*
[2]*Molecular Photoscience Research Center, Kobe University, Kobe 657-8501, Japan*

(Received 31 May 2012, Received in final form 26 July 2012, Accepted 9 August 2012)

Cantilever-detected high-frequency electron spin resonance (ESR) is a powerful method of sub-terahertz and terahertz ESR spectroscopy for a tiny magnetic sample at low temperature. In this technique, a small magnetization change associated with ESR transition is detected as deflection of a sample-mounted cantilever. So far, we have succeeded in ESR detection at 370 GHz using a commercial piezoresistive microcantilever. The spin sensitivity was estimated to ~10^{12} spins/gauss. In order to further increase the sensitivity, we adopt a fiber-optic-based detection system using a Fabry-Perot interferometer in place of piezoresistive system. Fabry-Perot cavity is formed between an optical-fiber end and microcantilever surface, and a change in the interference signal, corresponding to the cantilever deflection, is sensitively detected. This system is suitable for low-temperature and high-magnetic-field experiments because of its compact setup and less heat dissipation. In this study, performance of Fabry-Perot interferometer is evaluated, and its application to cantilever-detected ESR measurement is described.

Keywords : electron spin resonance, microcantilever, fabry-perot interferometer, terahertz wave

1. Introduction

Electron spin resonance (ESR) is widely used as a powerful technique for material analysis in order to probe local spin properties. Very often, the resonance condition of ESR absorption is given by the relation $g\mu_B H = h\nu$, in which g is the g factor, μ_B is the Bohr magneton, H is the applied magnetic field, h is the Planck constant, and ν is frequency of the applied electromagnetic wave. From detailed analysis of g factor, it is able to obtain microscopic insights into the local electronic states because g factor and line width are sensitively affected by the local crystal field or neighboring magnetic interactions.

To perform quantitative analysis, it is important to separate individual ESR signal from multiple absorption lines. For this purpose, ESR measurement in high-frequency range is very useful, since the Zeeman energy splitting can be large enough to resolve individual ESR absorptions. This is of particular importance for ESR study of magnetic samples such as transition metal oxides where ESR line width is often broad due to strong exchange interactions.

Experimentally, high-sensitivity ESR measurements are performed using a commercial X-band ESR spectrometer. The sensitivity is extremely high, typically on the order of ~10^9 spins/gauss. In this technique, however, microwave frequency is almost fixed, and it is difficult to extend the frequency region beyond W-band.

On the other hand, high-frequency ESR is usually carried out with a transmission method. An electromagnetic wave is introduced into the sample location using an oversized waveguide, and a change in the transmitted intensity is monitored. In this method, the operating frequency can be changed by replacing the light source, since an oversized waveguide is used. However, this method has a relatively low sensitivity (~10^{15} spins/gauss), compared to that of X-band ESR system. As a result, transmission-type ESR experiments need a large-volume (> 10 mg) sample. In this sense, it is quite difficult to satisfy both high-frequency and high-sensitivity detection in ESR measurement. These limitations motivated us to develop an alternative method of high-frequency and high-sensitivity

*Corresponding author: Tel: +81-78-803-5656
Fax: +81-78-803-5770, e-mail: ohmichi@harbor.kobe-u.ac.jp

This paper was presented at the ICM2012, Busan, Korea, July 8-13, 2012.

ESR.

Recently, we have developed a new high-frequency and high-sensitivity ESR technique using a microcantilever [1-5]. In this method, a tiny sample is attached on a cantilever beam, and uniform magnetic field $\boldsymbol{H}$ is swept. When ESR condition is satisfied, sample magnetization $\boldsymbol{M}$ is changed, and resultant change of magnetic torque defined by $\boldsymbol{\tau} = \boldsymbol{M} \times \boldsymbol{H}$ is detected as cantilever deflection. This method has several advantages. (1) Multi-frequency measurement is possible because an oversized waveguide is used in a similar manner to the transmission method. (2) A very small sample (~1 μg) is measurable because of the small size of microcantilever. (3) Compared to the transmission technique, spin sensitivity is 3-6 orders of magnitude improved. So far, we have achieved ESR detection at 80-370 GHz using Gunn oscillator and backward travelling wave oscillator (BWO) as a light source. The spin sensitivity was estimated to 10^9 and 10^{12} spins/gauss at 80 and 370 GHz, respectively.

In the previous study, we used commercial piezoresistive cantilever [6]. Compared to optical detection system, piezoresistive cantilever is a self-sensing device and cantilever deflection can be easily measured by resistance measurement. This feature is a great advantage in low-temperature and high-field conditions. However, product lineup is very limited, and it is difficult to choose optimal cantilevers for each experimental setup. Besides, from viewpoint of sensitivity, piezoresistive detection is less sensitive than optical detection, in particular for low-temperature operation where heat dissipation has to be avoided.

Therefore, in order to achieve better sensitivity, optical detection combined with an optimal cantilever is strongly desired. For this purpose, a new detection system based upon fiber-optic interferometer is developed in this study. In this article, details of our interferometer design and performance evaluation of Fabry-Perot interferometer is described.

2. Fabry-Perot Interferometer

Cantilever deflection is detected by Fabry-Perot interferometer as shown in Fig. 1. Fabry-Perot cavity is formed between an optic-fiber end and microcantilever surface. A change in the cavity length *d,* corresponding to the cantilever deflection, is detected with a photodiode as a change in the interference signal. The relation between the signal voltage V and cavity length d is given by

$$V = V_0\left(1 - A\cos\left(\frac{4\pi d}{\lambda}\right)\right) \quad (1)$$

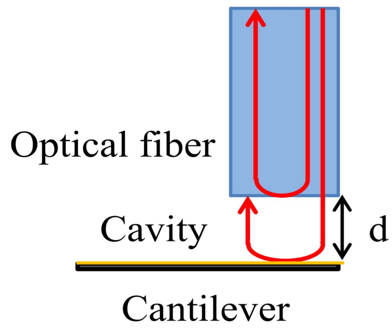

Fig. 1. (Color online) Principle of fiber-optic-based Fabry-Perot interferometer. Fabry-Perot cavity is formed between an optical-fiber end and the cantilever surface.

where $A = (V_{max} - V_{min})/(V_{max} + V_{min})$, $V_0 = (V_{max} + V_{min})/2$, and λ is laser wavelength. The most sensitive positions are easily obtained as $d = \lambda/8$, $3\lambda/8$, $5\lambda/8$. At these positions, a relation between the voltage change ΔV and displacement Δd is given as

$$\Delta V = 4\pi A V_0 \frac{\Delta d}{\lambda} \quad (2)$$

In order to realize optimal conditions, cavity length is usually adjusted using a piezo actuator. Instead, we adopt a fiber-coupled tunable laser in this study. By doing so, experimental setup and sample holder design become very simple.

Laser light irradiated by a fiber-coupled tunable laser is first fed into an optical isolator (40 dB) to prevent back-reflection to the laser module. Subsequently, the light is split by an optical coupler (Thorlabs, 10202A-90) with a ratio 90:10. The low-power branch is introduced to a liquid helium cryostat, and Fabry-Perot interferometer is formed at the fiber end, as explained above. The reflected

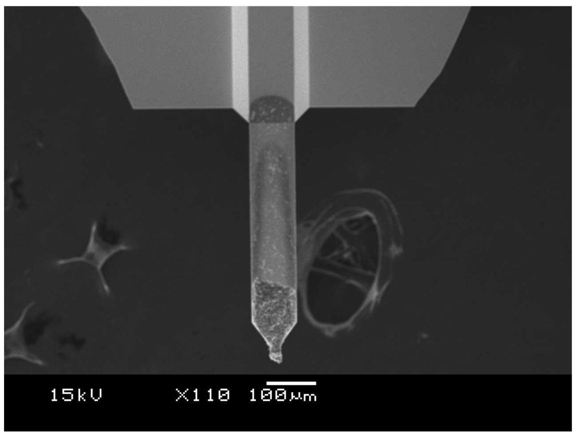

Fig. 2. SEM microscope image of a microcantilever used in this study. The cantilever beam is coated by gold in order to increase reflectance.

light from the cavity is transmitted to a photodiode with the optical coupler again.

In order to suppress back-reflection, APC connectors were used at all fiber connections. Besides, a bend-insensitive single-mode fiber is used to decrease the effect of thermal drift and vibration. A tunable laser (Agilent Technologies, 81989A) covers wavelength 1465-1675 nm, which is wide enough to cover several interference fringes. The maximum power of the laser was 10 mW, and coherence length was about $L_c = 6$ m with active coherence control. We used a commercial cantilever, as shown Fig. 2 (Nanoworld, ARROW-TL1Au). Gold-coated surface plays a role in high-reflectance mirror. Its dimensions of the cantilever were $500 \times 100 \times 1$ μm^3 and corresponding eigenfrequency is 6 kHz. Spring constant is 0.03 N/m, which is two orders softer than that of piezoresistive cantilever we previous used.

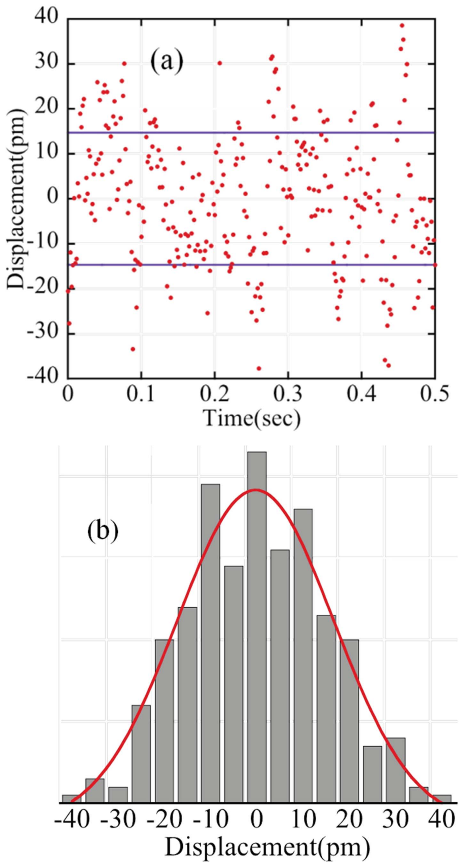

Fig. 3. (Color online) (a) Background noise measurement of Fabry-Perot interferometer. In this measurement, Fabry-Perot cavity was formed between an optical-fiber end and a fixed gold mirror. Measurements were carried out at room temperature. Laser wavelength was 1551 nm. Straight lines indicate the standard deviation of 15 pm. Fig. 3(b) Histogram of the noise voltage derived from Fig. 3(a). A red curve denotes the fitted result with Gaussian function.

3. Performance Evaluation of Fabry-Perot Interferometer

Here, we show performance of the Fabry-Perot interferometer system. Finesse of our interferometer was $F = 0.65$, which corresponds to an average round trip $n_{ave} = 1.04$. Indeed, the observed interference fringes are sinusoidal as expected. Low finesse was suitable for relatively large displacement case, at the expense of the sensitivity.

Background noise level was measured with a successive 0.5-s sampling of a photodiode signal, as shown in Fig. 3(a). In this experiment, Fabry-Perot interferometer is formed between an optical-fiber end and a fixed mirror. Fig. 3(b) shows a histogram of noise signals. The distribution curve was fitted by the Gaussian function and the half width at half maximum gives a standard deviation of 15 pm. This noise level is small enough for cantilever detected ESR measurement.

Fig. 4 represents thermal vibration spectrum of a cantilever measured by a spectrum analyzer. In this setup, Fabry-Perot cavity is formed between an optical-fiber end and cantilever surface at room temperature and in vacuum. Here, thermal vibration peak is clearly visible at $f = 5.7$ kHz, which corresponds to the cantilever eigenfrequency. At lower frequency side, two sharp peaks at 2 and 3 kHz are observed. The origin of these peaks is ascribed to coherence control of the laser. Although all optical components are placed on a vibration-free table, low frequency noises are not negligible below $f < 1$ kHz.

Spring constant of the cantilever can be estimated from Fig. 4. According to ref. [7], a cantilever is treated as a

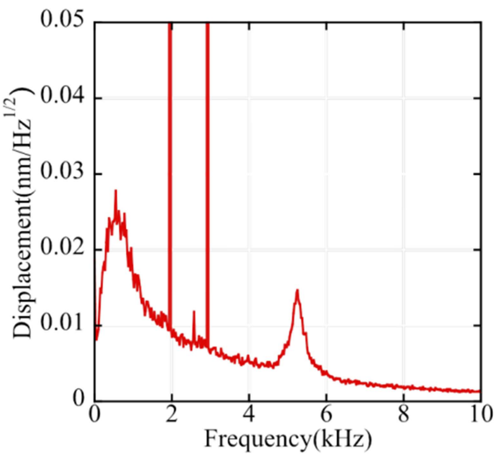

Fig. 4. (Color online) Thermal vibration spectrum of a cantilever. In this setup, Fabry-Perot interferometer was formed between an optical-fiber end and the cantilever surface. Measurements were carried out at room temperature and in vacuum. Laser wavelength was 1558.8 nm.

one-dimensional harmonic oscillator with a spring constant k, which is given by the following equation

$$k = \frac{k_B T}{\langle x^2 \rangle} = \frac{k_B T}{P} \tag{3}$$

where k_B is the Boltzmann constant, T is temperature, x is amplitude of cantilever displacement, and P is square measure of the thermal noise power spectrum. Using this equation, the estimated spring constant was k = 0.033 N/m, which is close to the spring constant of k = 0.03 N/m given in the data sheet.

4. ESR Detection System

ESR detection system combined with above-mentioned optical system was constructed, as shown in Fig. 5. A sample holder can be inserted into a variable temperature insert (1.5-200 K) with a sample bore of 35 mm. A superconducting magnet generates a static magnetic field of up to 15 T. A backward travelling wave oscillator (BWO) is used as a quasi-continuous light source. A combination of multiple BWO tubes covers a wide frequency range 200-1200 GHz.

BWO is placed 1.5 m away from the 15 T superconducting magnet because a permanent magnet is used inside BWO. An electromagnetic wave generated by BWO horizontally propagates in a copper light pipe, and is reflected by a polished copper mirror at the cryostat top. Subsequently, the electromagnetic wave is introduced via a polished stainless tube and is focused by a brass horn at the end of the light pipe. A sample-mounted cantilever is located at the horn end. In order to reduce transmission loss, the diameter of the light pipe is 16 mm. The diameter of horn end is typically 3 mm, which corresponds to a cut-off frequency of 80 GHz.

Optical modulation technique, where the intensity of an electromagnetic wave is modulated using a mechanical chopper, is used. Corresponding synchronized magnetization change at ESR absorption is detected using a lock-in amplifier. The maximum modulation frequency is 1000 Hz in this setup, which is limited by the revolution speed and the slit width of the chopper blade. Namely, slit width has to be larger than the wave length. The revolution speed is stabilized by a PLL circuit, which is controlled by an external local oscillator. Its synchronized TTL signal is fed into a lock-in amplifier as a reference signal. Since a tunable laser is used in our setup, a piezo actuator is not necessary. This compact design will be of particular importance when this technique is applied to magnetic resonance force microscopy (MRFM) in terahertz region, in which sample approach mechanism is additionally needed.

Figure 6 shows ESR absorption spectrum of Co Tutton salt which is a paramagnet with strong uniaxial anisotropy. In this setup, Gunn oscillator was used instead of BWO and the operating frequency was 120 GHz. Since the optimal condition was not reached, the signal-to-noise ratio is not so high. However, the spin sensitivity of ~10^{11} spins/gauss is obtained. Misalignment of the optical fiber upon cooling is found to be crucial in the setup. So, further increase of the detection sensitivity will be possible with modified alignment mechanism.

As mentioned above, thermally induced cantilever oscillation is typically on the order of 10 pm at room temperature, which is further reduced to 1 pm at liquid helium temperature. Spin sensitivity also depends on the spring constant of cantilever, and would be improved by 2-3 orders of magnitude with use of softer cantilevers. Together with these parameters, spin sensitivity of our setup would be better than ~10^6 spins/gauss even in terahertz region. A dominant factor to restrict the sensitivity

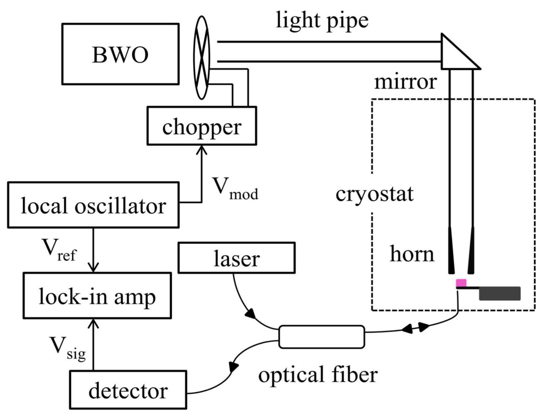

Fig. 5. (Color online) Schematic block diagram of cantilever-detected ESR measurement, combined with a fiber-optic interferometer.

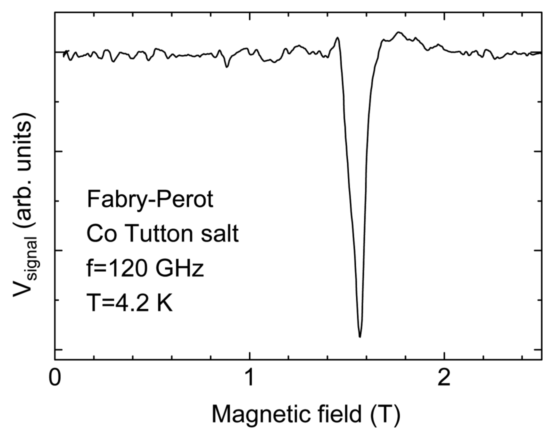

Fig. 6. ESR absorption spectrum of Co Tutton salt observed with the Fabry-Perot detection system.

is low output power of high-frequency light sources, which is less than 10 mW. If we adopt novel terahertz light sources such as gyrotron (> 10 W), further increase of the spin sensitivity will be possible.

4. Summary

We have constructed a cantilever detected ESR measurement system based on a fiber optic interferometer. The interferometer system described here has a better sensitivity than the piezoresisitive detection system, and standard deviation is obtained as 15 pm from noise measurement. Also, we were able to observe ESR signal with this setup. Use of a tunable laser makes experimental setup compact and simple, enabling further applications to MRFM in terahertz region.

Acknowledgments

One of the authors (Y. T.) acknowledges the financial support from the Motizuki Fund of Yukawa Memorial Foundation. This work was partly supported by a Grant-in-Aid for Scientific Research (B) (No. 22340101), and by a Grant-in-Aid for Challenging Exploratory Research (No. 23654103).

References

[1] E. Ohmichi, N. Mizuno and H. Ohta, Rev. Sci. Instrum. **79**, 103903 (2008).
[2] E. Ohmichi, N. Mizuno, T. Osada, and H. Ohta, Rev. Sci. Instrum. **80**, 013904 (2009).
[3] H. Ohta and E. Ohmichi, Appl. Mag. Res. **37**, 881 (2010).
[4] E. Ohmichi, N. Mizuno, S. Hirano, and H. Ohta, J. Low Temp. Phys. **159**, 276 (2010).
[5] Y. Tokuda, S. Hirano, E. Ohmichi, and H. Ohta, J. Phys. Conf. Ser. **400**, 032103/1-4 (2012).
[6] E. Ohmichi and T. Osada, Rev. Sci. Instrum. **72**, 3022 (2002).
[7] J. L. Hutter and J. Bechhoefer, Rev. Sci. Instrum. **64**, 1868 (1993).